# Supporting Information

## Combining surface chemical functionalization with introducing reactive oxygen species boosts ethanol electrooxidation

Jinjuan Zhao, Junhao Shu, Jiaxiao Wang, Jianqi Meng, Honglei Yang, Zhengping Dong* and Shuwen Li*

State Key Laboratory of Applied Organic Chemistry (SKLAOC), Key Laboratory of Advanced Catalysis of Gansu Province, College of Chemistry and Chemical Engineering, Lanzhou University, Lanzhou 730000, P. R. China

*Corresponding authors

**E-mail**: lishw@lzu.edu.cn (Shuwen Li), Dongzhp@lzu.edu.cn (Zhengping Dong)

**Address**: Tianshui South Road 222, Lanzhou 730000, P. R. China.

Supplementary information consists of 6 pages, including this page.

**Contents**: 2 Figures and 5 Tables.

## 1 Electrochemical sections

### 1.1 Preparation of the working electrodes

Firstly, the glassy carbon electrode (GCE, diameter = 3 mm) was polished with $Al_2O_3$ slurries and ultrasonically cleaned with water and ethanol. Then, 4.0 mg of catalysts were dissolved in 4.0 mL of co-solvents of Nafion (5 wt%), ethanol and water (Nafion : ethanol : water = 45 : 45 : 10, v : v : v), and ultrasonically treated for 25 min to form a black ink. Finally, 5 μL of the black ink was slowly spun-coated on the surface of clean GCE. The working electrodes were obtained after drying at room temperature. Based the contents of Pd in the electrocatalysts, the mass of Pd(loading) for calculating specific activity are 0.5000, 0.7175, 0.7450, 0.7290 and 0.7345 μg for Pd/C, Pd/GS, Pd/FGS, Pd-$CeO_{2-x}$/GS and Pd-$CeO_{2-x}$/FGS, respectively.

### 1.2 The CO stripping voltammetry experiments

First, high-purity $N_2$ was injected into the 1.0 M KOH electrolyte for 15 min to remove the oxygen in the electrolyte. Next, CO was bubbled into the above solution for 20 min at a potential of 0.6 V (*vs.* Hg/HgO). Finally, high-purity $N_2$ was bubbled into the CO-saturated electrolyte for 15 min to eliminate the dissolved CO in the electrolyte. The CO stripping curves were recorded using cyclic voltammetry at a scan rate of 50 mV $s^{-1}$.

### 1.3 Calculation of electrochemically active surface areas

In consideration of a certain amount of absorbed hydrogen penetrates into the interior of the Pd lattice space leading to error, the specific electrochemically active surface areas (ECSA) of the catalysts can be applicably acquired by integrating the reduction peaks of PdO based on the Equation S1.

$$ECSA = \frac{Q_s}{Q_{PdO} \times m_{Pd}} \quad \text{(Equation S1)}$$

Where $Q_s$ is the coulombic charge calculated by integrating the reduction peak area of PdO, $Q_{pdO}$ is estimated as 0.424 mC $cm^{-2}$ and assumed a charge required for the reduction of PdO monolayer and $m_{Pd}$ is Pd loading on the electrode surface.

## 2 Figures

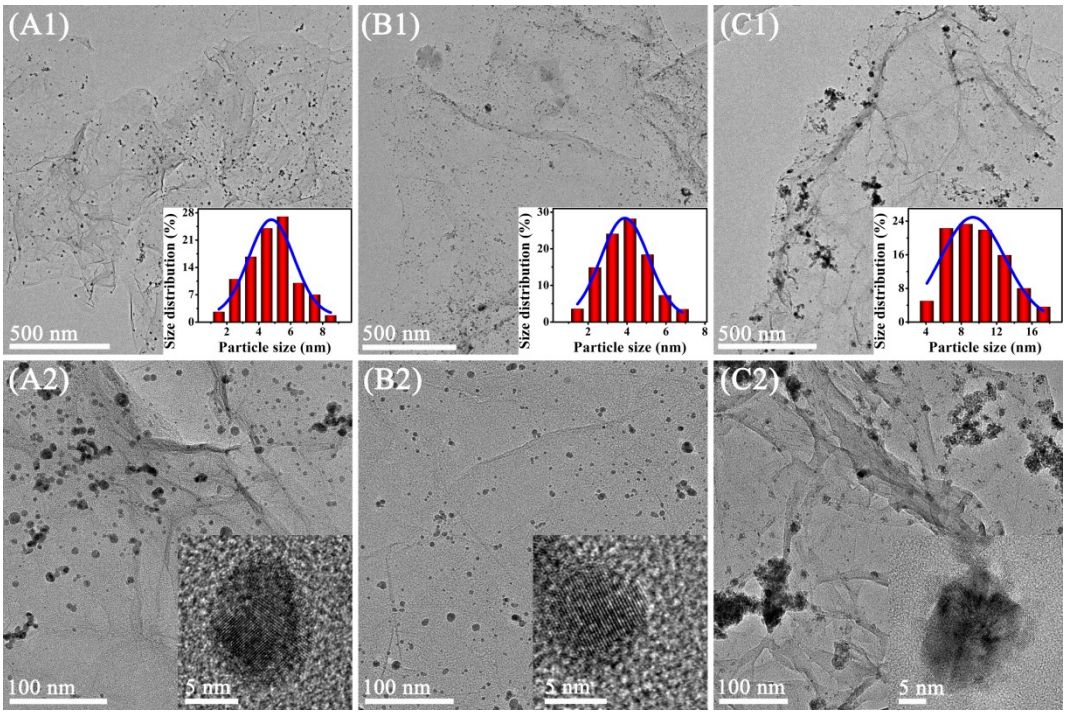


**Fig. S1** TEM images of Pd/GS (A1, A2), Pd/FGS (B1, B2) and Pd-$CeO_{2-x}$/GS (C1, C2). The insets are HRTEM images and the corresponding particle size statistical charts.

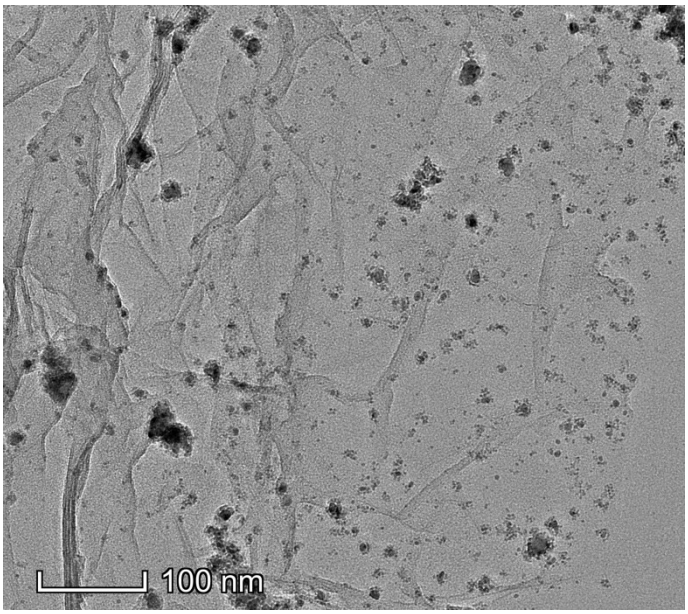


**Fig. S2** TEM image of Pd-$CeO_{2-x}$/FGS after 500 cycles CV scans.

## 3 Tables

**Table S1** The weight percentages of N, Ce and Pd in the obtained-catalysts.

| Catalysts | N (wt. %) | Ce (wt. %) | Pd (wt. %) |
|---|---|---|---|
| Pd/GS | - | - | 14.35 |
| Pd/FGS | 0.41 | - | 14.90 |
| Pd-$CeO_{2-x}$/GS | - | 3.58 | 14.58 |
| Pd-$CeO_{2-x}$/FGS | 0.36 | 3.60 | 14.69 |

**Table S2** Ce 3d analysis of the catalysts by XPS.

| Samples | $Ce^{4+}$ | | | $Ce^{3+}$ | | |
|---|---|---|---|---|---|---|
| | $^aE_B$/eV | | | $^aE_B$/eV | | |
| Pd-$CeO_{2-x}$/GS | 917.1 | 901.6 | 882.8 | 904.5 | 898.8 | 885.7 |
| Pd-$CeO_{2-x}$/FGS | 916.8 | 901.1 | 882.6 | 904.2 | 898.6 | 885.6 |

$^aE_B$ is binding energy.

**Table S3** Pd 3d analysis of as-prepared catalysts by XPS.

| Samples | $^aE_B$(eV) Pd(0) | | $^aE_B$(eV) $PdO_x$ | |
|---|---|---|---|---|
| | Pd $3d_{5/2}$ | Pd $3d_{3/2}$ | Pd $3d_{5/2}$ | Pd $3d_{3/2}$ |
| Pd/GS | 335.5 | 340.8 | 337.5 | 342.9 |
| Pd/FGS | 335.3 | 340.6 | 337.1 | 343.0 |
| Pd-$CeO_{2-x}$/GS | 335.5 | 340.8 | 337.1 | 343.6 |
| Pd-$CeO_{2-x}$/FGS | 335.4 | 340.7 | 337.1 | 342.7 |

$^aE_B$ is the binding energy.

**Table S4** The electrochemical performance of the tested-catalysts.

| Catalysts | ECSA ($m^2\ g^{-1}$) | $j'_f$ (mA $cm^{-2}$) | $j_f$ (mA $mg^{-1}$) | $j_s$ (mA $mg^{-1}$) | Retention ratio (%) |
|---|---|---|---|---|---|
| Pd/C | 20.4 | 1.92 | 390.7 | 7.7 | 12.2 |
| Pd/GS | 28.1 | 3.37 | 947.6 | 27.4 | 16.7 |
| Pd/FGS | 32.7 | 3.53 | 1809.7 | 63.7 | 18.8 |
| Pd-$CeO_{2-x}$/GS | 33.3 | 5.62 | 1871.3 | 77.7 | 19.9 |
| Pd-$CeO_{2-x}$/FGS | 37.7 | 7.04 | 2655.6 | 96.3 | 22.6 |

**Table S5** Comparison of the electrocatalytic activity of this work with recent reports[1-12].

| Catalysts | $j_f$ (mA $mg^{-1}$)[a] | Reference |
|---|---|---|
| Pd-$CeO_{2-x}$/FGS | 2655.8 | This work |
| Pd@PdAg bi-pyramids | 2517 | 1 |
| Pd NPs@Ni SAC | 1093 | 2 |
| $Pd_8$ Bi NPs | 2020 | 3 |
| Pd/BNCF-800 | 1989.2 | 4 |
| Pd-NS-CTAB | 2145 | 5 |
| Au@PdAu CNCs/C | 863 | 6 |
| Pd/Al-Mg-Ag | 1971.3 | 7 |
| $Pd_{0.5}Cu_{0.5}$ | 414.3 | 8 |
| $Pd_9Pb_1$ NPs | 2620 | 9 |
| L-Pd aerogel | 2310 | 10 |
| Ordered $PdNi_{0.3}Cu_{2.7}$ | 2100 | 11 |
| Pd/BNC-50 | 2638.41 | 12 |

[a]The electrochemical parameters was acquired in 1.0 M KOH and 1.0 M $C_2H_5OH$ solution at a scan rate of 50 mV $s^{-1}$.

## References

[1] J. Huang, Q. Liu, Y. Yan, N. Qian, X. Wu, L. Ji, X. Li, J. Li, D. Yang, H. Zhang, Nanoscale Adv. 4 (2022) 111-116.

[2] S. Li, A. Guan, H. Wang, Y. Yan, H. Huang, C. Jing, L. Zhang, L. Zhang, G. Zheng, J. Mater. Chem. A 10 (2022) 6129-6133.

[3] X. Lao, M. Yang, X. Sheng, J. Sun, Y. Wang, D. Zheng, M. Pang, A. Fu, H. Li, P. Guo, ACS Appl. Energ. Mater. 5 (2022) 1282-1290.

[4] Y. Su, C. Li, L. Xu, J. Xue, W. Yuan, C. Yao, J. Liu, M. Cheng, S. Hou, J. Alloys Compd. 901 (2022) 163333.

[5] M. Yang, M. Pang, J. Chen, F. Gao, H. Li, P. Guo, ACS Appl. Mater. Inter. 13 (2021) 9830-9837.

[6] G. Zhang, Y. Ma, X. Fu, W. Zhao, F. Liu, M. Liu, Y. Zheng, CrystEngComm 23 (2021) 2582-2589.

[7] S. Roy Chowdhury, J.C. Bhangoji, T. Maiyalagan, S.S. Shendage, Int. J. Hydrogen Energy 46 (2021) 4036-4044.

[8] P.C. Ashly, S. Sarkar, S.C. Sarma, K. Kaur, U.K. Gautam, S.C. Peter, J. Power Sources 506 (2021) 230168.

[9] L. Zang, J. Yan, M. Pang, B. Zhang, J. Chen, P. Guo, Langmuir 37 (2021) 13132-13140.

[10] R. Zhang, L. Zhu, X. Liu, J. Zhu, Y. Zhao, ACS Sustain. Chem. Eng. 9 (2021) 7837-7845.

[11] R. Jana, A. Datta, S. Malik, Chem. Commun. 57 (2021) 4508-4511.

[12] Y. Su, C. Li, C. Yao, L. Xu, J. Xue, W. Yuan, J. Liu, M. Cheng, S. Hou, Materials Today Energy 20 (2021) 100628.